A Laccase-Wiring Redox Hydrogel for Efficient Catalysis of O_2 Electroreduction

Nicolas Mano,* Valentine Soukharev, and Adam Heller

Department of Chemical Engineering and Texas Materials Institute, The University of Texas at Austin, Austin, Texas 78712

Received: October 4, 2005; In Final Form: February 23, 2006

Laccase was earlier wired to yield an O_2 electroreduction catalyst greatly outperforming platinum and its alloys. Here we describe the design, synthesis optimization of the composition, and characterization of the +0.55 V (AgAgCl) laccase-wiring redox hydrogel, with an apparent electron diffusion coefficient (D_{app}) of 7.6×10^{-7} cm^2 s^{-1}. The high D_{app} results in the tethering of redox centers to the polymer backbone through eight-atom-long spacer arms, which facilitate collisional electron transfer between proximal redox centers. The O_2 flux-limited, true-area-based current density was increased from the earlier reported 560 to 860 μA cm^{-2}. When the O_2 diffusion to the 7-μm-diameter carbon fiber cathode was cylindrical, half of the O_2 flux-limited current was reached already at 0.62 V and 90% at 0.56 V vs Ag/AgCl, merely −0.08 and −0.14 V versus the 0.7 V (Ag/AgCl) reversible O_2/H_2O half-cell potential at pH 5.

Introduction

Redox hydrogels constitute the only electron-conducting phases in which the permeation of water-soluble biological reactants and products, including water-soluble biochemicals, ions, and electrons, are all rapid. Their rapid permeation enables the transport of electrons between electrodes and multiple layers of redox enzymes. The three-dimensional hydrogels obviate the need of orienting the enzyme molecule on electrode surfaces, which is otherwise required to reduce the electron-transfer distance and allow electron exchange between enzymes and electrodes.[1−5] The hydrogels electrically wire the reaction centers of co-immobilized enzymes to electrodes, and absence of leachable components from the wired enzyme electrodes allows their use in the body, in flow cells, and in miniature, compartmentless biofuel cells, such as the glucose−O_2 cell, where glucose is electrooxidized to gluconolactone, and O_2 is electroreduced to water.[6−9] The transport of electrons through redox polymers is measured by their apparent electrons diffusion coefficients, D_{app}. The coefficient can be determined by electrochemical impedance spectroscopy,[10,11] by measuring the transient currents passing through the polymer coated electrodes when the potential is stepped,[12−20] or by measuring the steady-state currents using interdigitated microelectrode arrays (IDAs).[14,21−27]

Electrons can diffuse in redox polymers by several mechanisms, including percolation between immobile redox centers, collision of mobile reduced and oxidized redox centers and, in some polymers also by electron or hole conduction through a conjugated backbone.[1,14,28,29] In the absence of conjugated backbone conduction and unless the polymer is so heavily loaded with redox centers that the percolation is rapid, the dominant cause of conduction is collisional electron transfer between reduced and oxidized redox centers tethered to the polymer backbone. Because the rate of electron transferring collisions increases with the mobility of the tethered redox centers, the greater their mobility, the faster the electrons diffuse.[30] The segmental mobilities increase upon solvation of the polymer, decrease upon its cross-linking, and are reduced by attractive Coulombic, hydrogen-bonding, dipolar, or induced dipolar interactions between segments, known to raise the glass transition temperature. The Dahms−Ruff theory describes charge transport by electron hopping between freely diffusing redox centers. Blauch and Saveant[31,32] developed a bounded diffusion model, predicting D_{app} for polymers when the displacement of the redox centers is rapid and extensive. According to the model

$$D_{app} = \frac{((k_{ex}(\delta^2 + 3\lambda^2) C_{RT}))}{6} \quad (1)$$

where k_{ex} is the solution-phase self-exchange rate of the redox species, δ is the characteristic electron-hopping distance, the distance across which the tethered redox center can actually move is λ, and C_{RT} is the concentration of the redox species. When the redox centers are well-attached to the polymer and their physical diffusion does not contribute to electron transport[33,34]

$$D_{app} = \frac{k_{ex}\,\delta^2\,C_{RT}}{6} \quad (2)$$

The equation can be regarded as the extreme limit of eq 1, with $D_{phys} = 0$ (where D_{phys} represents physical diffusion in the absence of electron hopping). The reported apparent electron diffusion coefficients in redox hydrogels in equilibrium with aqueous solutions range between 10^{-12} and 10^{-6} cm^2 s^{-1}. Forster and co-workers systematically investigated electron transport in redox hydrogel films, [35−38] exemplified by poly(4-vinylpyridine), with part of the pyridines coordinated with $[Os(bpy)_2Cl]^{+/2+}$.[16,17,39,40] The D_{app}, typically of $\sim 10^{-9}$ cm^2 s^{-1} [37] in H_2SO_4 and in 1 M NaCl,[35,39] depended on the nature of the

* Corresponding author. E-mail: mano@mail.utexas.edu.

10.1021/jp055654e CCC: $33.50
Published on Web 05/18/2006

SCHEME 1: Synthetic Route to Polymer I

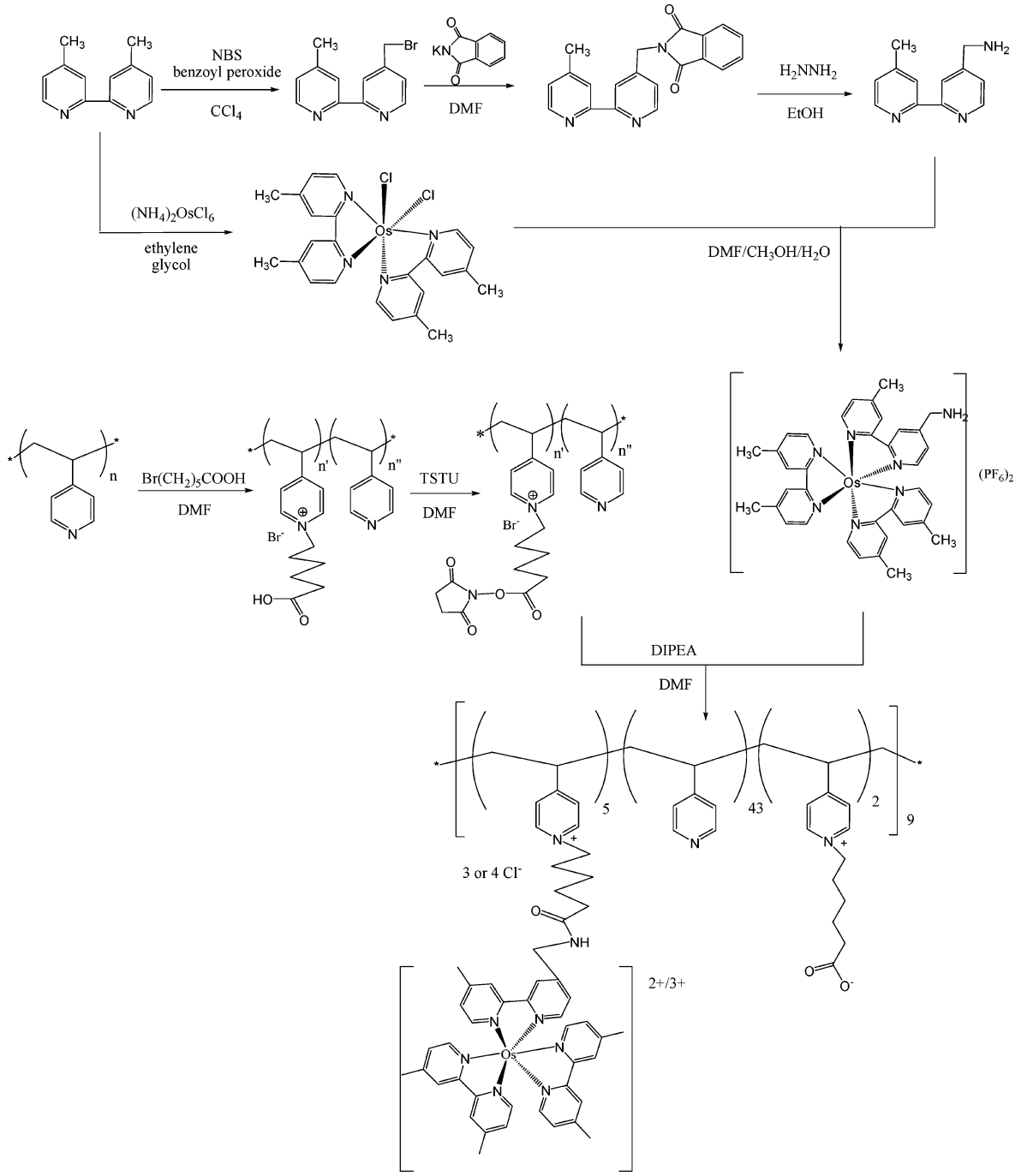

(A) H_2O, 40-50 °C, 24 h. (B) NaH/methyl *p*-toluenesulfonate, DMF, 0 °C to room temperature, 4 h. (C) $(NH_4)_2OsCl_6$ (0.5 equiv), ethylene glycol, 140 °C, 24 h. (D) NaH (1.1 equiv)/CH_3I (1.0 equiv), DMF, 0 °C to room temperature, overnight. (E) NaH/*N*-(6-bromohexyl)phthalimide/NaI, DMF, 80 °C, 24 h. (F) H_2NNH_2, EtOH, reflux, 24 h. (G) Ethylene glycol, 140 °C, 24 h. (H) Chloride resin/H_2O/Air, 24 h. (I) NH_4PF_6/H_2O. (J) 6-Bromohexanoic acid/DMF, 90 °C, 24 h. (K) TSTU/*N*,*N*-diisopropylethylamine, DMF, 7−8 h. (L) *N*,*N*-Diisopropylethylamine, DMF, rt, 24 h. (M) Chloride resin/H_2O, 24 h. (N) Ultrafiltration.

electrolyte and its concentration, on the temperature, and on the density of redox centers. Sirkar and Pishko[41] reported a D_{app} value as low as 2×10^{-12} cm^2 s^{-1} for a hydrogel based on the copolymer of poly(ethylene glycol) diacrylate and vinylferrocene in a phosphate buffer solution. Komura et al.[42] reported $D_{app} \sim 2 \times 10^{-10}$ cm^2 s^{-1} for the conjugated nonredox polymer poly(*N*,*N*′-bis(3-pyrrol-1-yl-propyl)-4,4′-bipyridinium) chloride in aqueous 0.2 M NaCl. Bu and co-workers[43] reported D_{app} values between 6×10^{-8} and 6×10^{-7} cm^2 s^{-1} for redox hydrogels made by copolymerizing vinylferrocene, acrylamide, and *N*,*N*′-methylenebisacrylamide. In conjugated redox polymers based on the complexation of poly(2-(2-bipyridyl)-bibenzimidazole) with bis(2,2′-bipyridyl) Ru^{2+} or bis(2,2′-bipyridyl) Os^{2+}, Cameron and co-workers[10,11] reported $D_{app} \approx 10^{-8}$ cm^2 s^{-1} in acetonitrile with 0.1 M Et_4NClO_4. For the conjugated nonredox polymers polypyrrole and poly(1-methyl-3-pyrrol-1-methyl pyridinium), Mao reported $D_{app} \approx 10^{-8}$ cm^2 s^{-1}.[44] The two highest D_{app} values, 1.7×10^{-6} cm^2 s^{-1} and 6×10^{-5} cm^2 s^{-1} were reported by Murray and co-workers,[45,46] respectively, for poly-[$Os(bpy)_2(vpy)_2$] sandwiched between a Pt and a porous Au

SCHEME 2: Structure of PVI-[Os(2,2′,6′,2″-terpyridine)-(4,4′-dimethyl-2,2′-bipyridine)$_2$]Cl$_2$

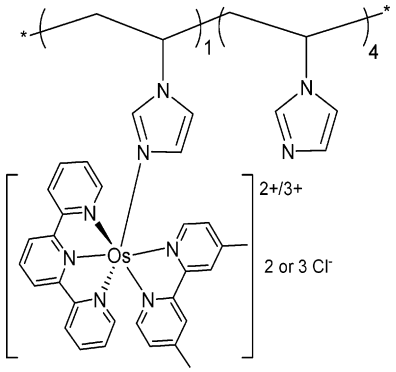

electrode bathed in dry N_2 and for doped poly(benzimidazobenzophenanthroline).

Because the model of Blauch and Saveant (eq 1) predicted that D_{app} should scale in redox hydrogels with the square of the length of the tethers binding the redox centers to the backbones, we synthesized earlier an enzyme wire[6,47] with 13-atom-long flexible tethers binding the redox centers to the backbone. Because the enzyme wired was glucose oxidase, the tethered redox centers were dialkylated biimidazole complexes of $Os^{2+/3+}$. Their redox potential was −0.2 V/ AgAgCl, only 0.16 V positive to the redox potential of the FAD/$FADH_2$ cofactor of GOx at pH 7.2.[48] The long tethers increased the frequency of effective electron-transferring collisions between reduced and oxidized osmium centers in chloride and other solutions, making D_{app} as large as 6×10^{-6} cm^2 s^{-1}.[47,49]

Here we describe the synthesis and characteristics of the earlier reported laccase-wiring +0.55 V/AgAgCl redox hydrogel with a relatively high D_{app} in a pH 5 aqueous citrate buffer solution. It contains eight-atom-long tethers between its redox centers and its backbone. To probe the effect of the tether, we compare its electrochemical characteristics with those of a +0.55 V/AgAgCl redox hydrogel with a short tether, PVI-[Os(2,2′,6′,2″-terpyridine)(4,4′-dimethyl-2,2′-bipyridine)$_2$]Cl]$_2$. We also reconfirm that the bioelectrocatalyst outperforms platinum in the catalysis of electroreduction of O_2 to water.

Experimental Section

Synthesis of PVP-[Os(4,4′-dimethyl-2,2′-bipyridine)$_2$(4-aminomethyl-4′-methyl-2,2′-bipyridine)Cl]$^{2+/3+}$. *4-Phthalimidylmethyl-4′-methyl-2,2′-bipyridine.* A mixture of 4,4′-methyl-2,2′-bipyridine (1.84 g, 10 mmol), *N*-bromosuccinimide (1.9 g, 10.7 mmol), and benzoyl peroxide (100 mg) in carbon tetrachloride (50 mL) was refluxed for 20 h. The reaction mixture was cooled on ice for 1 h and filtered to remove the red precipitate. The solvent was removed, and the residue containing 4-bromomethyl-4′-methyl-2,2′-bipyridine (MS: *m*/*z* 264 (M^+)) as a major product was dissolved in 80 mL of *N*,*N*-dimethylformamide. Potassium phthalimide (3 g, 16.2 mmol) was added, and the reaction mixture was stirred at 40 °C for 1 h under argon atmosphere. To the mixture was added 250 mL of distilled water, and the mixture was extracted with dichloromethane (150 mL × 3). The organic layer was collected, dried over Na_2SO_4, and concentrated. The residue was purified by running it through neutral alumina using ethyl acetate/hexane (10 → 50%) as the eluent to yield white crystalline solid (0.5 g, 15%). MS: *m*/*z* 330 (M^+). ^{1}H NMR ($CDCl_3$, δ): 2.45 (3H, s), 4.7 (2H, s), 7.20 (1H, d), 7.29 (1H, d), 7.49 (2H, m), 7.85(2H, m), 8.20 (1H, s), 8.35 (1H, s), 8.60 (1H, d), 8.94 (1H, d).

4-aminomethyl-4′-methyl-2,2′-bipyridine. The solution of 4-phthalimidylmethyl-4′-methyl-2,2′-bipyridine (0.3 g, 0.91 mmol) and hydrazine hydrate (0.3 mL, 6.12 mmol) in 40 mL of EtOH was refluxed for 7 h and then cooled to room temperature and poured into 100 mL of brine. The solution was basified to pH 12 with 2 M NaOH aq and extracted with CH_2Cl_2 (50 mL × 3). The combined organic layers were dried over Na_2SO_4 and concentrated in vacuo. The product was purified with alumina column chromatography ($CHCl_3$/MeOH/isopropylamine = 90/9/1) to yield pale-yellow oil (0.15 g, 82%). MS: *m*/*z* 200 (M^+). ^{1}H NMR ($CDCl_3$, δ): 2.31 (s, 3H), 2.70 (s, 2H), 4.15 (s, 2H), 7.00 (m, 1H), 7.10 (m, 1H), 8.16 (br s, 1H), 8.25 (br s, 1H), 8.51−8.57 (m, 2H).

[Os(4,4′-dimethyl-2,2′-bipyridine)$_2$(4-aminomethyl-4′-methyl-2,2′-bipyridine)](PF$_6$)$_2$. The complex [Os(4,4′-dimethyl-2,2′-bipyridine)$_2$Cl$_2$][50] (0.38 g, 0.6 mmol) was dissolved in a mixture of methanol (10 mL), DMF (10 mL), and water (10 mL). The ligand 4-aminomethyl-4′-methyl-2,2′-bipyridine (0.12 g, 0.6 mmol) was added to the solution, which was refluxed under nitrogen for 36 h. After cooling to room temperature and filtration, 150 mL of water was added, and the solution was poured slowly into a rapidly stirred NH_4PF_6 solution (5 g in 100 mL H_2O). The precipitate was collected and redissolved in 30 mL of acetonitrile and precipitated again from NH_4PF_6 solution (3 g in 150 mL H_2O). The dark-green precipitate was collected by filtration, washed with water (40 mL × 3) and ether (40 mL × 3), and dried in vacuo at 40−50 °C for 24 h (0.5 g, 80%).

Poly(4-(N−(5-carboxypentyl)pyridinium)-co-4-vinylpyridine) was synthesized by a reported method,[47] except that the poly(4-vinylpyridine) used had an average molecular weight of 50 000 instead of 160 000. ^{1}HNMR (DMSO-d_6, δ): 8.72 (br s, 2.0H), 8.23 (br s, 11.6H), 7.46 (br s, 2.0H), 6.56 (br s, 11.2H), 4.45 (br s, 2.0H), 1−2.3 (br m, 28.4H). The number of protons given for each peak is relative, providing integration ratios between the polymer protons, and shows that about 15% of pyridine units was quaternized by 6-bromohexanoic acid.

Polymer I. To a dry DMF suspension of poly(4-(*N*-(5-carboxypentyl)pyridinium)-*co*-4-vinylpyridine) (75 mg) *O*-(*N*-succinimidyl)-*N*,*N*,*N*′,*N*′-tetramethyluronium tetrafluoroborate (27 mg, 90 μmol) was added, the mixture was stirred for 15 min, and then *N*,*N*-diisopropylethylamine (14.5 μL, 155 μmol) was added. After stirring the reaction mixture for 8 h, [Os(4,4′-dimethyl-2,2′-bipyridine)$_2$(4-aminomethyl-4′-methyl-2,2′-bipyridine)](PF$_6$)$_2$ (130 mg, 124 μmol) was added slowly, followed by 14.5 μL of *N*,*N*-diisopropylethylamine. The solution was stirred for 24 h and then poured into 100 mL of EtOAc. The solvent was removed by decanting, and the precipitate was redissolved in 10 mL of CH_3CN. To the solution was added BioRad AG 2-X8 chloride exchange resin and 100 mL of water. The resulting mixture was stirred for 24 h, filtered, and dialyzed with H_2O by an ultramembrane filtration under 70 psi argon pressure, using Millipore polyethersulfone membrane with a molecular weight cutoff of 10 000. The dialyzed polymer was lyophilized to yield a brown solid. Yield: 0.16 g. Elemental analysis: C 70.6, H 7.3, N 12.1. Accordingly, the ratio between free pyridine, carboxypentyl-pyridine, and pyridine with osmium complex units of the polymer is approximately 43:5:2.

Other Chemicals and Materials. AG1 × 4 chloride resin was purchased from Bio-Rad Laboratories, Hercules, CA. All other chemical reagents were purchased from Aldrich Chemicals, Co. Deionized water was used for the synthesis and analysis. All of the electrochemical measurements were performed in a citrate buffer solution (pH 5, 0.2 M). The solutions

were made with deionized water that was passed through a purification train (Sybron Chemicals Inc, Pittsburgh, PA). Poly(ethylene glycol) (400) diglycidyl ether (PEGDGE) was purchased from Polysciences Inc., Warrington, PA. The synthesis of the redox polymer PVI-[Os(2,2′,6′,2″-terpyridine)(4,4′-dimethyl-2,2′-bipyridine)$_2$]Cl$_2$ (polymer **II**) was previously reported.[2,51,52]

Instrumentation and Analysis. The ^{1}H NMR spectra were recorded with a Varian Inova-500 spectrometer (500 MHz), and elemental analyses were performed by Quantitative Technologies, Inc., Whitehouse, NJ. The electrochemical experiments were performed by using a CH Instruments electrochemical detector model CHI832 bipotentiostat and a dedicated computer. Surfaces coverages of the modified electrodes were determined by integration of 1 mV·s^{-1} scan rate voltammetric waves of the osmium redox complexes and were based on the geometric areas of the 3-mm-diameter glassy carbon electrodes or the 25-μm-diameter platinum electrodes. The thicknesses of the dry and swollen redox polymer films were obtained from backscattered electron micrographs, obtained using an environmental scanning electron microscope (ESEM).[27,47]

The temperature was controlled with an isothermal circulator (Fisher Scientific, Pittsburgh, PA). The measurements were carried out in a water-jacketed electrochemical cell at 37.5 °C containing 50 mL of buffer. To maintain a fixed volume of solution in the cell, the bubbled gases were presaturated with water by passage through a bubbler, which also contained the pH 5 citrate buffer. The potentials were measured versus a commercial Ag/AgCl (3 M KCl) reference electrode. The counterelectrode was a platinum wire (BAS, West Lafayette, IN) and the 25-μm-diameter platinum microelectrode was from Cypress Systems, Lawrence, KS. Ultrapure argon was purchased from Matheson (Austin, TX).

Rotating Disk Electrodes. Vitreous carbon rotating disk electrodes (V-10 grade from Atomergic (Farmingdale, NY) of 3 mm diameter were prepared as reported.[12,13] They were polished sequentially with slurries of 5, 1, and 0.3 μm alumina particles (Buehler, Lake Bluff, IL), sonicated, and rinsed with ultrapure water. The cleaning process was repeated until no voltammetric features were observed in the potential range of interest, −0.4 to 0.4 V vs Ag/AgCl, in 50 mV/s scans in PBS. The total loaded amount of polymer and cross-linker was constant at 100 μg·cm^{-2}. After deposition and drying, the films were cured for at least 18 h at room temperature before the electrodes were used.

Pt Microelectrodes (25-μm Diameter). The electrodes were electrochemically cleaned by cycling in 0.1 M H_2SO_4 between potentials adequate to oxidize, then reduce, the platinum surface.[49] Excessive cycling was avoided in order to minimize the extent of surface roughening. A total of 15 mg/mL of the polymer solution was deposited by evaporation on the electrode surface. Upon hydratation, polymer **I** swells by a factor 2.4 and polymer **II** by a factor 2.3.[47] The polymer thicknesses were ∼36 μm for polymer **I** and ∼34.5 μm for polymer **II** for assumed densities of 1 g/cm^3.[15,47]

Carbon Fiber Electrodes. Prior to their coating, the 7-μm-diameter fibers (0.0044 cm^2) were made hydrophilic by exposure to 1 Torr O_2 plasma for 3 min.[53] The cathodic catalyst were made by published procedures[2,8,54] One cathodic catalyst consisted of the cross-linked adduct of 45.6 wt % laccase, 47.2 wt % redox polymer **I**, and 7.2 wt % PEGDGE, and the other of the 40 wt % laccase, 52.8 wt % redox polymer **II**, and 7.2 wt % PEGDGE.

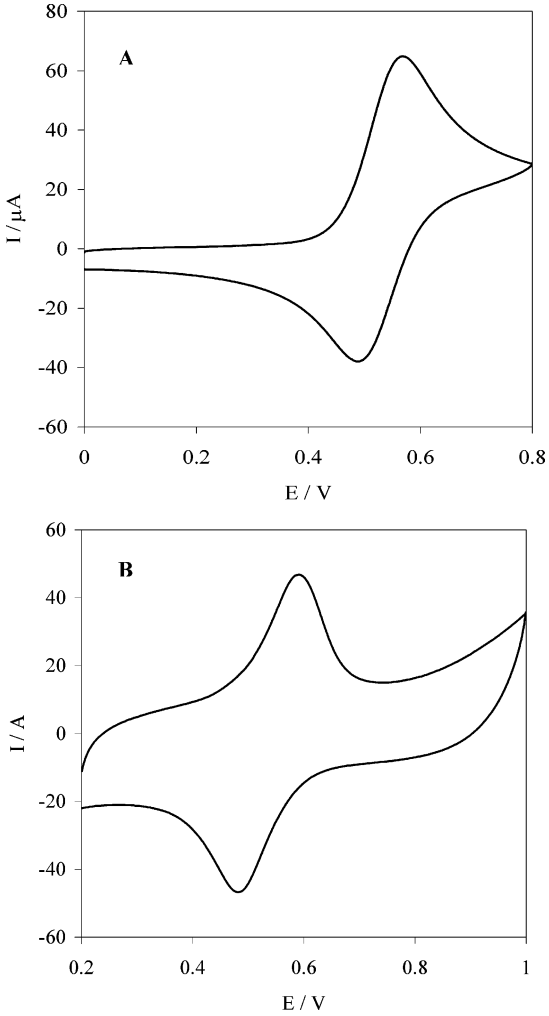

Figure 1. Cyclic voltammograms of polymers **I** (A) and **II** (B) on 3-mm-diameter glassy carbon electrodes under argon; 0.2 M citrate buffer pH 5, 37 °C, 20 mV·s^{-1}.

Results

Figure 1A shows the cyclic voltammograms of polymer **I**, and Figure 1B shows the cyclic voltammograms of polymer **II** under argon (3-mm-diameter glassy carbon electrode, pH 5 0.2 M citrate buffer, 37 °C). The voltammograms are characteristic of polymer-bound osmium complexes with redox potentials of +550 mV vs Ag/AgCl. At the 20 mV s^{-1} scan rate, the voltammogram of polymer **I** exhibited a symmetrical wave with 65 mV peak separation; the separation for polymer **II** was >110 mV.

Figure 2 shows the dependence of the apparent diffusion coefficients of polymer **I** (solid circles) and polymer **II** (open circles) on the cross-linker concentration. Each value shown is the average of five measurements. Upon increasing the cross-linker concentration from 0 to 25 wt %, the apparent diffusion coefficient of polymer **I** decreased by about 8-fold, from 7.6 × 10^{-7} to 1 × 10^{-7} cm^2 s^{-1}. The apparent coefficient diffusion of polymer **II** did not change significantly with the concentration of the cross-linker, decreasing from 6.2 × 10^{-9} to 5.6 × 10^{-9} cm^2 s^{-1}.

Figure 3 shows the shifts of the peak at half-height, E_{whm}, upon increasing the cross-linker weight percent. For polymer **I**, E_{whm} was 90 mV at ∼1 wt % cross-linker content, increasing to ∼135 mV at 25 wt %. For polymer **II**, E_{whm} was 120 mV at low ∼1 wt % cross-linker content, increasing to ∼145 mV at 25 wt %.

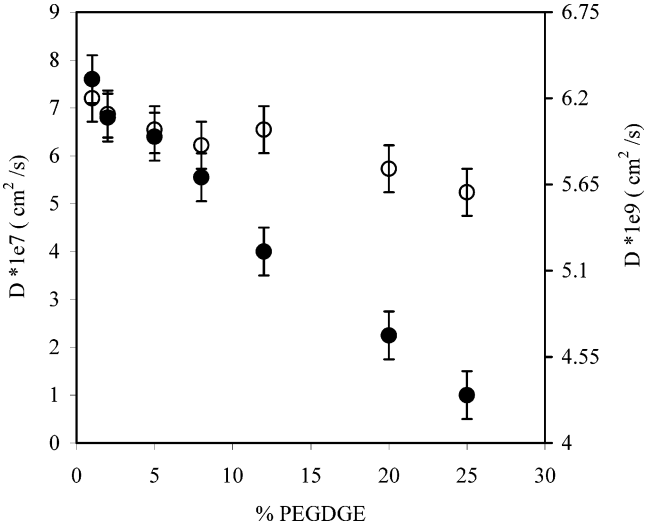

Figure 2. Dependence of D_{app} of polymer **I** (solid circles, left axis) and polymer **II** (open circles, right axis) on the weight fraction of the PEGDGE cross-linker; 25-μm-diameter platinum electrode. Other conditions as in Figure 1.

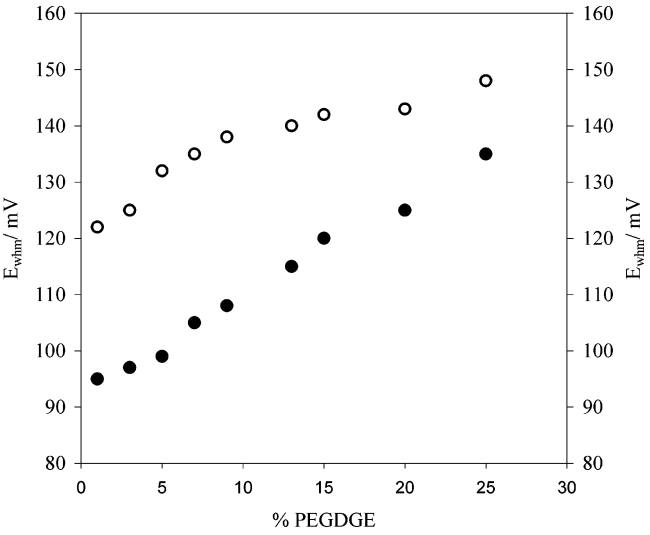

Figure 3. Dependence of the peak width at half-height, E_{whm} for polymer **I**, (solid circles, right axis) and polymer **II** (open circles, left axis) on the weight fraction of the cross-linker PEGDGE; 25-μm-diameter platinum electrode. Other conditions as in Figure 1.

Figure 4 shows the optimal composition (polymer/laccase/cross-linker) for the bioelectrocatalysts made with polymer **I** (solid circles) and polymer **II** (open circles) in a 0.2 M pH 5 citrate buffer through the 0−60 wt % range. In the first group of experiments, the cross-linker (PEGDGE) weight percentage was fixed at 7 wt %, and the total loading of all film components was fixed at 0.8 mg cm^{-2}. Between 5 and 40 wt %, the current density increased with the weight percentage of laccase, reaching a current density of 0.6 mA·cm^{-2} at 40 wt % laccase for polymer **II** and reaching a current density of 0.8 mA·cm^{-2} at ∼46 wt % laccase for polymer **I**. Above these weight percentages, the current density declined rapidly. Precipitation, attributed to the formation of a neutral electrostatic adduct between the cationic polymer and the enzyme (pH = 4), was observed above 60 wt % laccase. In experiments where the weight percent of the cross-linker was varied and the laccase/redox polymer weight ratio was kept constant, the optimal PEGDGE wt % was found to be 7.2. The resulting optimal catalysts were composed of 45.6 wt % laccase, 47.2 wt % redox polymer **I**, and 7.2 wt % PEGDGE, and 40 wt % laccase, 52.8 wt % redox polymer **II**, and 7.2 wt % PEGDGE **.**

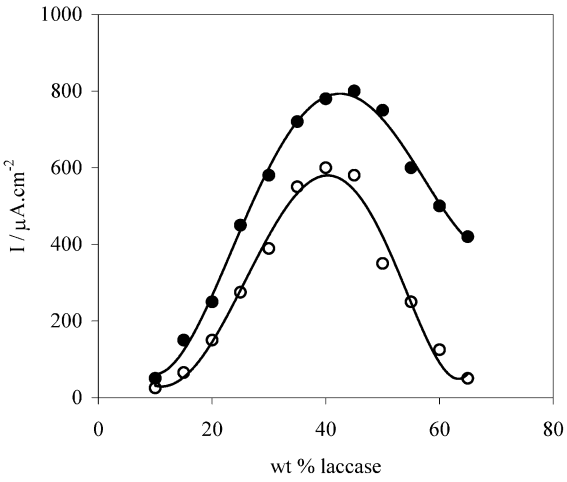

Figure 4. Dependence of the current density on the laccase weight percentage for the bioelectrocatalysts made with polymer **I** (solid circles) and with polymer **II** (open circles).

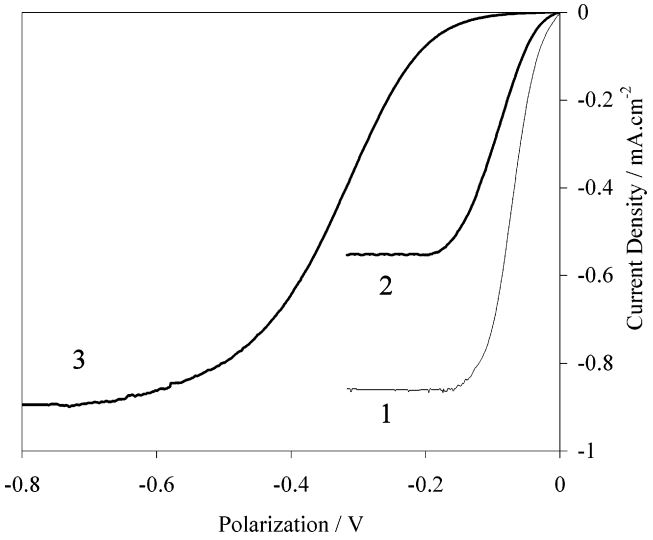

Figure 5. Polarizations of 7-μm-diameter, 2-cm-long carbon fiber cathodes modified with laccase wired by polymer **I** (with tether, curve 1), and polymer **II** (which has no tethers between its redox centers and its backbone, curve 2). The cathode was coated with a film containing 45.6 wt % laccase, 47.2 wt % redox polymer **I**, and 7.2 wt % PEGDGE; or containing of 40 wt % laccase, 52.8 wt % redox polymer **II**; or 7.2 wt % PEGDGE 45.6 wt % laccase, 47.2 wt % polymer **I**, and 7.2 wt % PEGDGE. 0.1 M pH 5 citrate buffer, quiescent solution, under air, 37 °C. Scan rate 1 mV s^{-1}. Polarization of a 6-μm-diameter, 2-cm-long smooth solid platinum fiber cathode in 0.5 M H_2SO_4 (curve 3). Quiescent solution, under air, 37 °C. Scan rate 1 mV s^{-1}.

The polarizations (potential versus the reversible potential of the O_2 /H_2O half-cell in the same electrolyte) of a miniature carbon fiber cathode (7 μm diameter, 2 cm long) modified with either the bioelectrocatalyst made with polymer **I** (Figure 5, curve 1) or polymer **II** (Figure 5, curve 2) in a quiescent pH 5 citrate buffer under air at 37.5 °C are compared in Figure 5. With polymer **I**, oxygen is electroreduced already at −20 mV, and a current density of 0.86 mA·cm^{-2} is reached at −0.2 V vs Ag/AgCl. With polymer **II**, the current density at −0.2 V vs Ag/AgCl is less, 0.58 mA·cm^{-2}. On the 6-μm-diameter platinum electrode, oxygen is electroreduced on the fiber at −120 mV, and a current density of 0.86 mA·cm^{-2} is reached at −0.8 V vs Ag/AgCl (Figure 5, curve 3).

Discussion

Design and Synthesis of Polymer I. The design of the +0.55 V vs Ag/AgCl potential redox polymer **I** followed that for the reported glucose oxidase "wiring" polymer.[47] The osmium complex, with two 4,4′-dimethyl-2,2′ -bipyridine ligands and one 4-aminomethyl-4′-methyl-2,2′-bipyridine ligand, was reacted to form amides, with *N*-(5-carboxypentyl) pyridinium functions of poly(4-vinylpyridine), (PVP), introduced by partially quaternizing PVP with 6-bromohexanoic acid. Unlike the earlier wires of laccase or bilirubin oxidase, in which the redox functions were coordinatively bound to ring nitrogens of backbone imidazoles, polymer **I** had eight-atom-long, flexible tethers between its Os complexes to its backbone. The redox function of polymer **I** is the (4,4′-dimethyl-2,2′-bipyridine)$_2$(4-aminomethyl-4′-methyl-2,2′-bipyridine) complex of $Os^{2+/3+}$; the redox potential of the complex is +0.55 V vs Ag/AgCl. This redox potential brought the redox potential of the hydrogel close to the redox potential of the type-1 copper centers of laccase, so that the electron transfer from the polymer to laccase was potential-wise downhill, but driven by the smallest necessary potential gradient, and thus maintaining the potential at which O_2 was reduced highly oxidizing.[55] The flexible spacer tethering the redox centers to the backbone was made eight atoms long, allowing effective electron-transferring collisions between the redox centers of the polymer and between polymer and enzyme redox centers, the tethered centers wiping overlapping volumes of the hydrogel. As a result, the apparent electron diffusion coefficient was high relative to that of other redox hydrogels.[12,13,30] In the redox centers of Polymer **I**, full coordination of the $Os^{2+/3+}$ by polydentate ligands provided the sought high self-exchange rate[56] and stability against ligand substitution encountered with monodentate ligands.[57]

Electrochemical Characteristics. Comparison of the characteristics of polymer **I** with those of polymer **II** having the same redox potential (+550 mV vs Ag/AgCl) but only a short tether (Figure 1B) shows that, with the long tether, the transport of electrons is enhanced: while the voltammogram of polymer **I** exhibited at 20 mV s^{-1} scan rate, a symmetrical wave, with only 65 mV separation of the anodic and cathodic peaks, the peak separation for polymer **II** was >120 mV.[58] Comparison of the peak separations suggested that D_{app} of polymer **I** was considerably higher than polymer **II**.

Apparent Electron Diffusion Coefficients. The apparent electron diffusion coefficient of a redox hydrogel is a function of (a) the structure of the redox polymer particularly, as seen, of the mobility of the redox functions; (b) the nature and diffusivity of the solution-phase anion, diffusing into the redox polymer and neutralizing the added positive charge when the polymer is oxidized and leaving the polymer when it is reduced; and (c) the cross-linking of the polymer, which reduces the mobility of its segments.

The apparent electron diffusion coefficients D_{app} were measured in a 0.2 M citrate buffer at 37 °C at 100 $\mu g \cdot cm^{-2}$ polymer loading. Details of the measurement procedures were reported earlier. In brief, the technique exploits the difference in the diffusion field at microelectrodes for different experimental time scales, i.e., linear versus radial diffusion at short versus long times. For long times, or slow scan rates, a steady-state plateau current is observed that is independent of the scan rate for $0.1 < \upsilon < 10$ mV s^{-1} because the thickness of the layer of the reduced or oxidized species that is depleted is comparable to the radius of the microelectrode, and the charge transport process is radial. The time-independent steady-state current, i_{ss}, is given by

$$i_{ss} = 4nFD_{app}C_{RT}r \tag{3}$$

where n is a number of electrons transferred, D_{app} is the apparent diffusion coefficient describing homogeneous charge transport through the deposit, C_{RT} is the effective concentration of Os^{2+} centers within the deposit, and r is the radius of the microelectrode. For short times, or fast scan rates, the depletion layer is significantly thinner than either the film thickness or the radius of the microelectrode, making the diffusion linear, and peaking voltammograms, reminiscent of dissolved redox species at macroelectrodes, are observed. In this case, D_{app} was derived of the voltammograms through the Randles−Sevcik equation[38,59] by plotting the voltammetric peak currents (i_p) versus the square root of the scan rates $\nu^{1/2}$

$$i_p = \frac{0.4463 \times nF^{3/2} \times A \times D_{app}{}^{1/2} \times C_{RT} \times \nu^{1/2}}{(RT)^{1/2}} \tag{4}$$

where n is the number of electrons transferred, F is the Faraday constant, R is the gas constant, T is the temperature, A is the area of the electrode, and C_{RT} is the effective electroactive site concentration.[58,60] The slope of the plots, which were, as expected, linear, provided the product ($D_{app}{}^{1/2}$ C_{RT}). By combining eq 3 and 4, the absolute value of D_{CT} and C_{RT} was determined. For polymer **II**, the product $D_{app}C_{RT}$ is $9.5 \times 10^{-12} \pm 0.5$ mol·cm^{-1} s^{-1} and the product $D_{app}{}^{1/2}C_{RT}$ is $1.2 \times 10^{-7} \pm 0.4$ mol·cm^{-2} $s^{-1/2}$. These yield a value of D_{app} of $6.2 \times 10^{-9} \pm 0.5$ cm^2 s^{-1}. For polymer **I**, D_{app} is $7.6 \times 10^{-7} \pm 0.5$ cm^2 s^{-1}. Evidently, the eight-atom-long flexible tethers allowed the redox centers to sweep large volume elements and increased the rate of electron-transferring collisions between the polymer segments. Although the centers were tethered, they were mobile within the volumes defined by their long tethers. The 120-fold increase in D_{app} could have been caused also by higher k_{ex} or C_{RT} (eq 1),[31,32] but the concentration of the redox centers was about the same in the two polymers, and it was unlikely that the k_{ex} of their $Os^{2+/3+}$ complexes varied by more than an order of magnitude. We attribute, therefore, the observed 120-fold increase in D_{app} to the 11-fold increase in λ, the physical displacement of the redox centers about their equilibrium positions, upon the eight-atom extension of the tether.

Covalent and Coordinative Cross-linking. As a redox polymer is increasingly cross-linked, whether electrostatically or covalently, its swelling is reduced. The gel becomes mechanically tough, and at the same time, as shown by Oh and Faulkner,[19] Bu,[43] and Rajagopalan,[12,14] the segments of its polymer become less mobile, and as a result, D_{app} decreases. As seen in Figure 3, D_{app} of polymer **I** decreases faster upon cross-linking than that of the already heavily electrostatically cross-linked polymer **II**. Neither of the two polymers was sheared off electrodes rotated for 20 h at 500 rpm in pH 5 citrate buffer at 37 °C while cycled between −0.4 and +0.1 V versus Ag/AgCl at 50 mV s^{-1}: the heights of the voltammetric peaks decreased only by 4% for both. This is in contrast with our previous results with a PVI-[Os(4,4′-diamino-2,2′-bipyridine)$_2$-Cl]$^{+/2+}$ redox hydrogel.[47] The difference is attributed to the coordinative cross-linking of the PVI-[Os(4,4′-diamino-2,2′-bipyridine)$_2$Cl]$^{+/2+}$ redox hydrogel by partial exchange of the inner-sphere chloride of its osmium complex by imidazoles of neighboring chains upon redox cycling.[61] The added cross-linking decreases the segmental mobility, the diffusivity of electrons, and thereby thickness of electroactive film. Because

the polymers of this study do not have an inner-sphere chloride, no coordinative cross-linking occurred, and the polymers were more stable under redox cycling. The tether did not stabilize or destabilize the redox hydrogel.

Composition. There are four electron-transfer steps in the wired-laccase-catalyzed electrooxidation of O_2. At steady state, the current associated with each step is necessarily the same. The currents flowing from the cathode to the polymer (1), through the redox hydrogel (2), from the polymer to the laccase molecules (3) and from laccase molecules to O_2, are all identical. The limit of each of these currents is defined by the polymer/enzyme ratio. The limits of (3) and (4) increase upon increasing the polymer/enzyme mass ratio, unless the electrostatic adduct between the polycationic polymer and the polyanonic enzyme precipitates. The polymer/enzyme mass ratio can be increased if the specific activity of the enzyme is higher and less enzyme is required in the optimal composition. If the apparent electron diffusion coefficient of the polymer is higher and less polymer mass is required, the ratio can be decreased. Increasing D_{app} thus allowed a decrease in the polymer/enzyme/cross linker ratio from 1.32 to 1. As in other wired enzyme films, cross-linking reduces D_{app} because the more rigid the gel, the less the segmental mobility and the frequency of effective collisions of the redox functions on which D_{app} depends. Because the eight-atom-long tethers increased D_{app} 120-fold, we were able to increase the PEGDGE cross-linker weight fraction to 7.2 wt %, from the earlier 5 wt %,[2,8] and form a leather-like, thick, and well-adhering cathodic gel.

Electrooreduction of O_2 to Water. The hydrated films of cross-linked polymer **I** constitute the best wires of laccase to date. Because the cathode was now close to being fully covered by the electrocatalytic film, the O_2 flux-limited current density increased from the earlier reported 560 μA cm^{-2} (Figure 5, curve 2), reached with polymer **I**, (PVI-spacer-[Os(2,2′,6′,2″-terpyridine-4,4′-dimethyl-2,2′-bipyridine)$_2$Cl]$^{2+/3+}$) to 860 μA cm^{-2} (Figure 5, curve 1). When the O_2 diffusion to the 7-μm-diameter carbon fiber cathode was cylindrical, half of the O_2 flux-limited current was reached already at 0.62 V and 90% at 0.56 V vs Ag/AgCl, merely −0.08 and −0.14 V versus the 0.7 V (Ag/AgCl) reversible O_2/H_2O half-cell potential at pH 5. To show that the laccase-containing hydrogel of polymer **I** was superior to platinum in electrocatalyzing the reduction of O_2 to water, we compared, at 37 °C, the polarizations (potential versus the reversible potential of the O_2 /H_2O half-cell in the same electrolyte) of the wired-laccase-coated 7-μm-diameter carbon fiber (in pH 5 citrate buffer), and of a 6-μm-diameter platinum fiber (in 0.5 M H_2SO_4) (Figure 5, curve 3). The Pt fiber reached 90% of the limiting 0.9 mA·cm^{-2} current density only at a polarization of −0.40 V, while the wired-laccase-coated fiber reached 90% of the limiting O_2 electroreduction current density at a polarization as small as −0.07 V.

Conclusion

The redox polymer described efficiently connects the laccase reaction centers to electrodes. Its redox potential allows poising of the O_2 cathode just 0.15 V negative to the redox potential of the laccase copper cluster at pH 5.[48] Its eight-atom-long flexible spacer arm increases the apparent coefficient of electron diffusion to 7.6×10^{-7} cm^2 s^{-1}, and the coordination of the $Os^{2+/3+}$ centers with three substituted bipyridines provides stability against ligand substitution. The reduced redox centers deliver electrons to laccase so rapidly and at such a small potential gradient that the electroreduction of O_2 to water is much better catalyzed than by the classical catalyst, platinum.

Acknowledgment. This study was supported by the Office of Naval Research (N00014-02-1-0144) and by the Welch Foundation. N.M. thanks The Oronzio de Nora Industrial Electrochemistry Fellowship of The Electrochemical Society.

References and Notes

(1) Heller, A. *J Phys. Chem. B* **1992**, *96*, 3579.
(2) Katz, E.; Buckmann, A. F.; Willner, I. *J. Am. Chem. Soc.* **2001**, *123*, 10752.
(3) Mano, N.; Kim, H.-H.; Zhang, Y.; Heller, A. *J. Am. Chem. Soc.* **2002**, *124*, 6480.
(4) Baldini, E.; Dall'Orto, V. C.; Danilowicz, C.; Rezzano, I.; Calvo, E. J. *Electroanalysis* **2002**, *14*, 1157.
(5) Katz, E.; Willner, I.; Kotlyar, A. B. *J. Electroanal. Chem.* **1999**, *479*, 64.
(6) Mano, N.; Mao, F.; Heller, A. *J. Am. Chem. Soc.* **2002**, *124*, 12962.
(7) Mano, N.; Mao, F.; Heller, A. *ChemBioChem* **2004**, *5*, 1703.
(8) Soukharev, V. S.; Mano, N.; Heller, A. *J. Am. Chem. Soc.* **2004**, *126*, 8368.
(9) Mano, N.; Mao, F.; Heller, A. *J. Am. Chem. Soc.* **2003**, *125*, 6588.
(10) Cameron, C. G.; Pickup, P. G. *J. Am. Chem. Soc.* **1999**, *121*, 11773.
(11) Cameron, C. G.; Pittman, T. J.; Pickup, P. G. *J. Phys. Chem. B* **2001**, *105*, 8838.
(12) Gregg, B. A.; Heller, A. *J. Phys. Chem.* **1991**, *95*, 5970.
(13) Gregg, B. A.; Heller, A. *J. Phys. Chem.* **1991**, *95*, 5976.
(14) Rajagopalan, R.; Aoki, A.; Heller, A. *J. Phys. Chem.* **1996**, *100*, 3719.
(15) De Lumley-Woodyear, T.; Rocca, P.; Lindsay, J.; Dror, Y.; Freeman, A.; Heller, A. *Anal. Chem.* **1995**, *67*, 1332.
(16) Forster, R. J.; Vos, J. G.; Lyons, M. E. G. *J. Chem. Soc., Faraday Trans.* **1991**, *87*, 3769.
(17) Forster, R. J.; Vos, J. G.; Lyons, M. E. G. *J. Chem. Soc., Faraday Trans.* **1991**, *87*, 3761.
(18) Forster, R. J.; Vos, J. G. *J. Electrochem. Soc.* **1992**, *139*, 1503.
(19) Oh, S.-M.; Faulkner, L. R. *J. Am. Chem. Soc.* **1989**, *111*, 5613.
(20) Oh, S.-M.; Faulkner, L. R. *J. Electroanal. Chem.* **1989**, *269*, 77.
(21) Goss, C. A.; Majda, M. *J. Electroanal. Chem.* **1991**, *300*, 377.
(22) Chidsey, C. E.; Feldman, B. J.; Lundgren, C.; Murray, R. W. *Anal. Chem* **1986**, *58*, 601.
(23) Feldman, B. J.; Murray, R. W. *Anal. Chem.* **1986**, *58*, 5844.
(24) Feldman, B. J.; Murray, R. W. *Inorg. Chem.* **1987**, *26*, 1702.
(25) Dalton, E. F.; Surridge, N. A.; Jernigan, J. C.; Wilbourn, K. O.; Facci, J. S.; Murray, R. W. *Chem. Phys.* **1990**, *140*, 143.
(26) Nishihara, H.; Dalton, F.; Murray, R. W. *Anal. Chem.* **1991**, *63*, 2955.
(27) Aoki, A.; Rajagopalan, R.; Heller, A. *J. Phys. Chem.* **1995**, *99*, 5102.
(28) Aoki, A.; Heller, A. *J. Phys. Chem.* **1993**, *97*, 11014.
(29) Heller, A. *Acc. Chem. Res.* **1990**, *23*, 128.
(30) Rajagopalan, R.; Heller, A. Electrical "wiring" of glucose oxidase in electrons conducting hydrogels. In *Molecular Electronics: A Chemistry for the 21st Century Monograph*; Jortner, J., Ratner, M., Eds.; Blackwell Science Ltd, Cambridge, MA, 1997; p 241.
(31) Blauch, D. N.; Saveant, J.-M. *J. Phys. Chem.* **1993**, *97*, 6444.
(32) Blauch, D. N.; Saveant, J.-M. *J. Am. Chem. Soc.* **1992**, *114*, 3323.
(33) Laviron, E. J. *J. Electroanal. Chem.* **1980**, *112*, 1.
(34) Andrieux, C. P.; Saveant, J.-M. *J. Electroanal. Chem.* **1980**, *111*, 377.
(35) Forster, R. J.; Kelly, A. J.; Vos, J. G.; Lyons, M. E. G. *J. Electroanal. Chem.* **1989**, *270*, 365.
(36) Forster, R. J.; Vos, J. G. *J. Chem. Soc., Faraday Trans.* **1991**, *87*, 1863.
(37) Forster, R. J.; Vos, J. G. *J. Electroanal. Chem.* **1991**, *314*, 135.
(38) Keane, L.; Hogan, C.; Forster, R. J. *Langmuir* **2002**, *18*, 4826.
(39) Forster, R. J.; Vos, J. G. *Electrochim. Acta* **1992**, *37*, 159.
(40) Forster, R. J.; Vos, J. G. *Langmuir* **1994**, *10*, 4330.
(41) Sirkar, K.; Pishko, M. V. *Anal. Chem.* **1998**, *70*, 2888.
(42) Komura, T.; Kijima, K.; Yamaguchi, T.; Takahashi, K. *J. Electroanal. Chem.* **2000**, *468*, 166.
(43) Bu, H.-Z.; English, A. M.; Mikkelsen, S. R. *J. Phys. Chem. B* **1997**, *101*, 9593.
(44) Mao, H.; Pickup, P. G. *J. Am. Chem. Soc.* **1990**, *112*, 1776.
(45) Jernigan, J. C.; Murray, R. W. *J. Am. Chem. Soc.* **1987**, *109*, 1738.
(46) Wilbourn, K.; Murray, R. W. *J. Phys. Chem.* **1988**, *92*, 3642.
(47) Mao, F.; Mano, N.; Heller, A. *J. Am. Chem. Soc.* **2002**, *125*, 4951.
(48) Stankovich, M. T.; Schopfer, L. M.; Massey, V. *J. Biol. Chem.* **1978**, *253*, 4971.
(49) Forster, R. J.; Walsh, D. A.; Mano, N.; Mao, F.; Heller, A. *Langmuir* **2004**, *20*, 862.
(50) Kober, E. M. *Inorg. Chem.* **1988**, *27*, 4587.

(51) Barton, S. C.; Kim, H.-H.; Binyamin, G.; Zhang, Y.; Heller, A. *J. Phys. Chem. B* **2001**, *105*, 11917.
(52) Barton, S. C.; Kim, H.-H.; Binyamin, G.; Zhang, Y.; Heller, A. *J. Am. Chem. Soc.* **2001**, *123*, 5802.
(53) Sayka, A.; Eberhart, J. G. *Solid State Technol.* **1989**, *32*, 69.
(54) Mano, N.; Fernandez, J. L.; Kim, Y.; Shin, W.; Bard, A. J.; Heller, A. *J. Am. Chem. Soc.* **2003**, *125*, 15290.
(55) Marcus, R. A. *J. Phys. Chem.* **1963**, *67*, 853.
(56) Ryabov, A. D. *Adv. Inorg. Chem.* **2004**, *55*, 201.
(57) Binyamin, G.; Chen, T.; Heller, A. *J. Electroanal. Chem.* **2001**, *500*, 604.
(58) Kim, H.-H.; Mano, N.; Zhang, Y.; Heller, A. *J. Electrochem. Soc.* **2003**, *150*, A209.
(59) Forster, R. J.; Vos, J. G. *J. Inorg. Organomet. Polym.* **1991**, *1*, 67.
(60) Bard, A. J.; Faulkner, L. R. *Electrochemical Methods. Fundamentals and Applications*, 2nd ed.; John Wiley & Sons: New York, 2001.
(61) Gao, Z.; Binyamin, G.; Kim, H.-H.; Barton, S. C.; Zhang, Z.; Heller, A. *Angew. Chem., Int. Ed.* **2002**, *41*, 810.